

Toxic Heavy Metal Ions Removal from Wastewater by Nano-Magnetite: Case Study Nile River Water

Shimaa M. Ali, A. Galal, Nada F. Atta, Yassmin Shammakh*

Chemistry Department, Faculty of Science, Cairo University, Giza 12613, Egypt.

NANO-MAGNETITE was used as an eco-friendly sorbent (without the usage of surfactants during the synthesis) for removing Pb(II), Cd(II) and Cr(III) from water and wastewater. A single 7 nm cubic phase for magnetite was ascertained by X-Rays diffraction (XRD) and high resolution transmission electron microscope (HRTEM). Field emission scanning electron microscopy (FESEM) image showed the agglomeration of magnetite particles upon adsorption. The Langmuir isotherm was used to estimate the maximum adsorption capacities of 576.4, 144.3 and 301.0 mg/g for Pb(II), Cd(II) and Cr(III), respectively. The adsorption mechanism followed a pseudo-second order kinetics. The studied competing cations and anions showed minor effects on the rate of adsorption. Magnetite with high adsorption ability adsorbed Pb(II), Cd(II) and Cr(III) from a ternary mixture as effectively as from their individual solutions. The presented sorbent can be regenerated by 1% HNO₃ with a recovery percent of 91.4 % and reused with an adsorption efficiency of 84.1 % compared to the freshly prepared magnetite. As an example of application, the nano-magnetite was used to decontaminate river water-samples from lead ions.

Keywords : Water decontamination, Nano-oxides, River water, Adsorption isotherm, Sorbent regeneration.

Introduction

Nano-sized metal oxides can be successively employed as effective sorbents for the removal of toxic heavy metal ions from wastewater. They provide high surface area and specific affinity for several pollutants. They also possess minimal environmental impact, low solubility and no secondary pollution have been reported upon their usage. Nano-sized metal oxides should satisfy the following criterions: nontoxicity, high sorption capacities and selectivity to relatively different concentrations of pollutants and be regenerate easily [1]. Magnetic nano-particles can be easily separated after adsorption process by applying a magnetic field. Moreover, the isolated magnetic sorbents can be regenerated and reused.

Nanospheres magnetite was used to adsorb Cr(VI) and Pb(II) from water effectively [2]. The adsorption capacities were 9 mg/g and 19 mg/g at pH values of 4 and 5 for Cr(VI) and Pb(II), respectively. Mixed maghemite-magnetite was

employed as sorbent for Cd(II) ions removal [3]. The uptake capacity of Cd(II) ions increased by increasing pH. Cadmium adsorption was due to a combined diffusion and electrostatic effects. The same magnetite maghemite mixture was used to remove arsenic and chromium by adsorption [4]. The maximum arsenic adsorption values were 3.69 mg/g for As(III) and 3.71 mg/g for As(V) at pH = 2, while for Cr(VI), 2.4 mg/g as was adsorbed at the same pH. In a previous work [5], magnetite and mixed magnetite-hematite nanoparticles were synthesized by different chemical methods such as combustion and coprecipitation then employed as sorbents for removal of Pb(II), Cd(II) and Cr(III) ions from water. It was found that the mixture composition, particle size, morphology and thus, the sorption ability was affected by the synthesis method. The coprecipitation method resulted in more efficient sorbents compared to combustion methods.

The objectives of this study are: to synthesize a single-phase nano-magnetite with an eco-

*Corresponding author e-mail: yassmin_shammakh83@hotmail.com

DOI : 10.21608/EJCHEM.2017.3583

©2017 National Information and Documentation Center (NIDOC)

friendly route and employ it for the removal of Pb(II), Cd(II) and Cr(III) ions from wastewater samples of south and central Delta Nile river; to determine both activation energy and mechanism of adsorption and to evaluate the effect of interference from some competing anions and cations on the adsorption process.

Experimental

Chemicals

All Chemicals were used as received: ferric nitrate nonahydrate ($\text{Fe}(\text{NO}_3)_3 \cdot 9\text{H}_2\text{O}$), ferrous chloride (FeCl_2), sodium hydroxide (NaOH), lead nitrate ($\text{Pb}(\text{NO}_3)_2$), ammonium hydroxide (NH_4OH), nitric acid (HNO_3), Chromium (III) chloride hexahydrate ($\text{CrCl}_3 \cdot 6\text{H}_2\text{O}$), cadmium bromide (CdBr_2), magnesium sulphate heptahydrate ($\text{MgSO}_4 \cdot 7\text{H}_2\text{O}$), sodium phosphate dodecahydrate ($\text{Na}_3\text{PO}_4 \cdot 12\text{H}_2\text{O}$) and calcium chloride (CaCl_2) were obtained from Aldrich (USA).

Synthesis of magnetite

Magnetite nanoparticles were prepared by the coprecipitation method in N_2 atmosphere. In summary, stoichiometric amounts of ferric/ferrous ions (molar ratio 2:1) were dissolved in deionized water. The pH of the solution was brought to a value of 10 by adding quantitatively 3M NaOH. A black precipitate is formed thereafter that was left to coagulate. The precipitate was washed with water, filtered and dried in air [5].

Adsorption experiment

Pb(II), Cd(II) and Cr(III) solutions were prepared from their corresponding stock solutions. The pH value was kept at 7 using 10^{-4} M NH_4OH and 10^{-4} M HNO_3 . For each of these solutions 0.4 g magnetite was added to one liter of each of the corresponding solution. The magnetite was dispersed by sonication for 30 min then was left in a rotating shaker (100 rpm) over night at room temperature. Each solution was then centrifuged at 3000 rpm for 15 min. The clear solution was collected and filtered through 0.2 μm cellulose-free syringe filters. After solution exposure to magnetite, the concentrations of lead, cadmium and chromium ions were measured using atomic absorption spectroscopy using a Zeenite 700P spectrometer (Analytical Jena).

The equilibrium concentration of adsorbed metal ion (q_e , mg/g) can be calculated from the following equation:

$$q_e = \frac{(C_0 - C_e)V}{W} \quad (1)$$

where, C_0 and C_e are the initial and equilibrium concentrations (mg/L) of metal ion in solution, V the volume (L), and W is the weight (g) of the adsorbent.

Structural and surface characterizations

The structure phases and average particle size of the synthesized magnetite was analyzed by XRD using Shimadzu XRD-700.

FESEM analysis and energy dispersive X-rays analysis (EDXA) were obtained using a Quanta FEQ 250 (accelerate voltage = 25 kV), HRTEM was performed using JEOL, JEM 2100 (accelerating voltage = 200 kV).

Sampling of waste-water from Nile River

Bottles used in sampling for both river water and wastewater were sterilized according to standard protocols. For the river samples the bottles were rinsed using water-stream three times before collecting the samples while for waste-water the samples were collected from a point where the waste-water is well mixed. The points of collection were determined to be near the center of the flow channel; this should be at approximately 40 to 60% of the water depth, where the turbulence is at a maximum so minimizing the possibility of solids settling.

Results and Discussion

Structural and surface characterizations

XRD

XRD was used to analyze the structural phases and the average particle size of the prepared magnetite before and after adsorption. It is important to confirm the structure of the resulting magnetite and to assess the possible changes to the structure before and after exposure to the polluted solutions. Data were compared with the ICDD card of magnetite (card number: 04-006-6550). Figure 1A shows the XRD patterns of magnetite (a) before adsorption and (b) after adsorption.

The results proved the successful incorporation of the Fe(III) at the Fe(II) cations sites confirming the formation of a single cubic phase of the synthesized magnetite and after exposure to the polluted solutions. Therefore, the adsorption process did not affect the structure of magnetite.

At this stage it could be suggested that the nano-magnetite can be used after regeneration while the structure is maintained. The low intensity of peaks in (b) indicates lack of crystallinity after the process of adsorption. This situation results from the adsorbed cations from the polluted solutions. The particle sizes of magnetite before and after adsorption were calculated from the XRD data according to the Scherrer equation [6] and were found to be 6.9 and 7.3 nm, respectively. These results suggest that the particles of magnetite increase in size after adsorption. This finding could be due to the further deposition of metallic particles collected from solution upon their adsorption onto the surface of the magnetite particles.

FESEM and HRTEM

The morphology of magnetite before and after adsorption was characterized by FESEM and HRTEM. Figure 1B shows HRTEM image of nano-magnetite reflecting well defined cubic symmetry of magnetite particles. Most particles have a size around 7 nm which agrees well with the particle size value calculated from XRD.

Figure 2 shows the FESEM images of

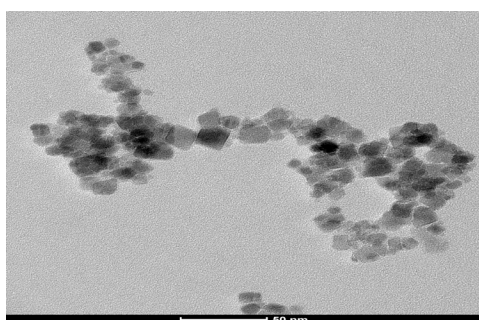
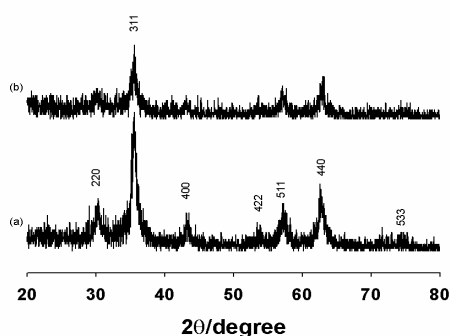


Fig.1. (A) XRD patterns of magnetite (a) before and (b) after adsorption, (B) HRTEM micrograph of magnetite before adsorption.

magnetite before (A) adsorption and after (B) adsorption. The agglomeration of magnetite particles after adsorption is clearly shown in the microstructures as the accumulation is mainly occurring at the edges of nano-particles. Again, these results are in good agreement with the increased particle size after adsorption as ascertained from XRD data.

EDAX

The elemental composition of magnetite before and after Pb(II) ions adsorption was determined by EDAX. Figures 2 (C and D) show the EDAX analyses; the results show dispersion peaks indicating the presence of Pb that again proves the adsorption its corresponding ions onto the nano-magnetite particles.

The EDAX spectrum for freshly prepared nano-magnetite particles showed the presence of Fe and O peaks (Fig.2C). Upon exposure of 0.4 g/L nano-magnetite to a solution containing 50 mg/L Pb(II) ions, the EDAX analysis of the particles revealed the presence of Pb peak as depicted in Figure 2D.

Adsorption isotherm

The effect of varying the initial metal concentration in the polluted solutions on the efficiency of adsorption was also studied. Thus, individual solutions containing different concentrations, ca. from 10-100 ppm, of each of Pb(II), Cd(II) and Cr(III) were used in this study. Figure 3A shows the effect of contaminant concentration on the adsorption efficiency of the nano-magnetite for each cation. The concentration range was selected to cover a relatively wide concentration range that would be acceptable for most of the worked standards for wastewater contamination in industrial urban regions.

It was noticed that in case of Pb(II) and Cr(III) ions, the adsorption efficiency is unaffected by the initial metal ion concentration, where average values of 99 and 99.8% were calculated for Pb(II) and Cr(III) ions, respectively. This indicates that the nano-magnetite can be used effectively for removal of these cations from polluted solutions with varying concentrations of the corresponding cations. A very slight decrease in the efficiency value was observed at high concentrations and it is more remarkable for the Pb(II) ion. On the other hand, the adsorption efficiency decreases with increasing the initial Cd(II) ion concentration.

While in case of Cd(II) ions, as the concentration

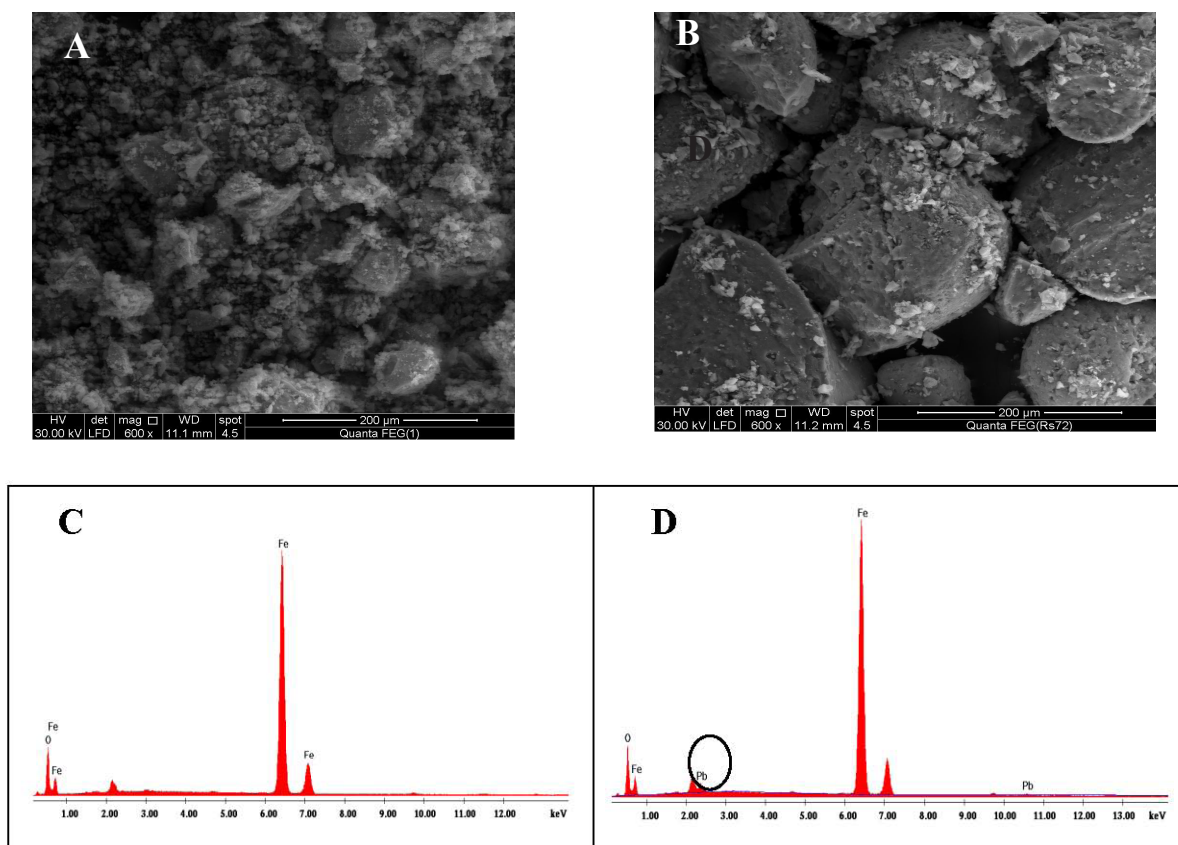


Fig. 2. FESEM micrographs of magnetite (A) before and (B) after the adsorption, the EDXA analysis of magnetite (C) before and (D) after the adsorption of Pb(II) ions.

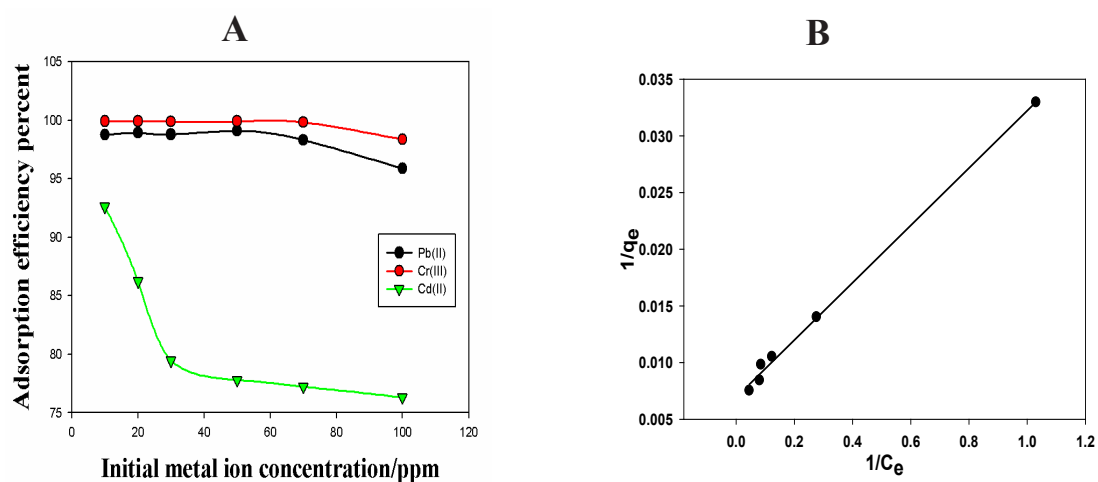


Fig. 3. (A) Variation of the adsorption efficiency with the initial metal ion concentrations for Pb(II), Cr(III) and Cd(II) ions and (B) langmuir isotherms for adsorption of Cd(II) on magnetite surface.

increases (up to 30 ppm) a decrease in adsorption efficiency of about 20% was observed. There is relatively slight decrease in the adsorption efficiency as the concentration of Cd(II) cations

increases from 40 to 100 ppm.

The most common models used to express adsorption are Freundlich and Langmuir isotherms

[7,8]. The adsorption isotherm experiments were performed on Pb(II), Cd(II) and Cr(III) on magnetite surface at 298 K. The results were correlated to both models and illustrated. The linearity in the plot of $1/q_e$ versus $1/C_e$ is depicted in Fig. 3B that realized the Langmuir model. The test for linearity of plot of $\ln(q_e)$ versus $\ln(C_e)$ (Freundlich model) failed compared to the Langmuir plot (Figure not shown). In the results of Fig. 3B, the data for Cd(II) adsorption are given. The values of Langmuir (KL, b) and Freundlich (k, n) constants were calculated and reported in Table 1. From the correlation coefficients estimated from the linear fit, the Langmuir model will be used in the study. The adsorption capacities of Pb(II), Cd(II) and Cr(III) on magnetite surface were listed in Table (2) and compared with other sorbents reported in literature.

Thus, magnetite has high adsorption capacity values of 576.37 mg/g, 144.34 mg/g and 301.02 mg/g for Pb(II), Cd(II) and Cr(III), respectively. The aforementioned values indicate that nano-magnetite has an excellent capacity for the studied metal ions removal from their corresponding solutions.

Kinetic study

The adsorption mechanism can be investigated by using pseudo-first-order and pseudo-second-order kinetic models [10] for Pb(II), Cd(II) and Cr(III) ions adsorption onto magnetite. We fitted the experimentally obtained results with two models; Lagergren pseudo-first-order and pseudo-second-order kinetic models according to

$$\log(q_e - q_t) = \log q_e - \frac{k_1}{2.303} t$$

$$\frac{1}{q_t} = \frac{1}{k_2 q_e^2} + \frac{1}{q_e} t$$

In these equations: q_t (mg g^{-1}) is the amount of adsorbed metal cation on the adsorbent at time t , and k_1 (min^{-1}) and k_2 ($\text{g mg}^{-1} \text{min}^{-1}$) are the corresponding rate constants.

According to the values of linear correlations of the plots of $\log(q_e - q_t)$ versus t , and (t/q_t) versus t (Fig. 4), a pseudo-second-order model is likely to account for the kinetics of the adsorption mechanism. This is correlated from the linear fit of straight lines obtained from the graphs shown in Fig. 4.

The successful application of the pseudo-

second-order model means that chemisorption can be used to explain the interaction between the magnetite and studied metal ions. However, at early adsorption stage, a physical interaction can be developed. Therefore, more than one mechanism can be used to express the adsorption process [31, 32].

We used the correlation coefficient from the linear plots of Fig. 4. Both kinetic models introduced above displayed linear relations. However, comparison of the r^2 values for both mechanisms showed higher value for the pseudo-second-order model. At the first stage of the adsorption process, a physical adsorption model is expected. At later stages, where phase changes are expected, a chemisorption process is expected which involves electron exchange between the solid phase and metal cations [31, 32].

Temperature effect

Adsorption experiments of the three studied metal ions, Pb(II), Cd(II) and Cr(III), onto magnetite were performed at different temperatures: 15, 25, 35, 45 and 55°C. Figure 5A shows the effect of temperature on the adsorption efficiencies of magnetite towards different metal ions.

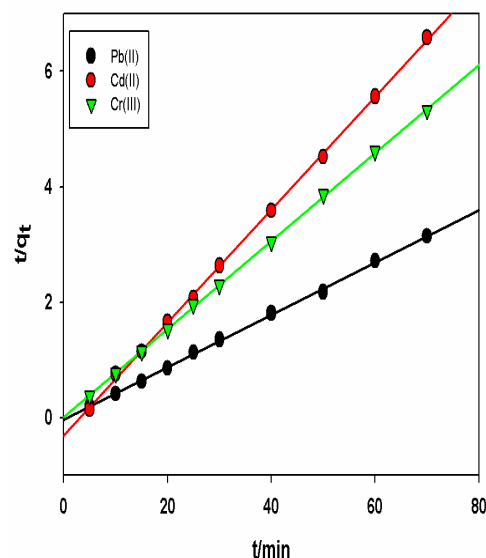


Fig. 4. Pseudo-second order Kinetic model of adsorption of Pb(II), Cd(II) and Cr(III) onto magnetite.

For the three metal ions studied, the adsorption efficiency increases with temperature. As depicted in Fig. 5A, the adsorption efficiencies increase from 85% to about 99% for Pb(II) ions, from 75% to about 98% for Cr(III) ions as the temperature spans from 15 °C to 35 °C. In case of Cd(II) ions the adsorption efficiency increases from 65% to about 77% within the same temperature span. The results indicate that the adsorption process is endothermic in nature; Table 3 lists the values of the heats of enthalpies calculated from the consecutive plots of Fig. 5(B). The magnetite prepared by the present coprecipitation method is porous in nature (5) that favors a diffusion controlled process if adsorbed ions through the pores of the nano-magnetite [33, 34].

The values of thermodynamics parameters, calculated from transition-states plots of Fig. 5 for different metal ions are recorded in Table 3 as described earlier [35]. The spontaneity of the adsorption process is indicated by the negative values of ΔG_0 . Since the adsorption increases with temperature rise, it is indicative of chemical adsorption [36].

Metal ions adsorption rate constants were determined as a function of temperature from the experimental data assuming pseudo second-order kinetics. A plot of $\ln K_2$ versus $1/T$ (Arrhenius plot) gives a straight line, with slope $-E_a/R$ and intercept of $\ln k$, (Fig. 5C). The magnitude of the activation energy can be used to determine the adsorption type whether physical or chemical. The activation energy values for Pb(II) and Cr(III) are 137.56 and 112.11 kJ/mol, respectively suggesting that Pb(II) and Cr(III) ions were chemically adsorbed onto the magnetite surface. While the value of activation energy for Cd(II) ions adsorption is 10.94 kJ/mol which means that the Cd(II) adsorption on magnetite is of physical nature rather than chemical [37, 38].

Interferences study

Effect of competing cations

Effects of many naturally occurring cations such as Na(I), Ca(II), and Mg(II) ions on the Pb(II) ions removal by magnetite nano-particles was investigated. Figure 6A shows the variation of the lead removal percent by magnetite with the concentration of the added competing cations.

The removal percent of Pb(II) ions decreases

noticeably from near 99% to about 94.7% upon increasing Ca(II) ions from 5 ppm to 40 ppm. Similar trend was also observed in presence of Mg(II) ions. The increase of Na(I) ions concentration within the same range, from 5 ppm to 40 ppm slightly decreases the adsorption percent of Pb(II) ions from 99.6% to about 99.2%. It was mentioned earlier that divalent cations are more strongly adsorbed when competing with monovalent cations because of their lower hydration energies [39]

Effect of interfering anions

Some naturally occurring anions such as chloride, sulfate, and phosphate may also cause interference in the removal of heavy metals. Thus, the effect of the coexistence of these anions on the removal of Pb(II) by the magnetite was also investigated. Various concentrations of aforementioned anions were added to 10 ppm Pb(II) ions solutions. The variation of the removal percent of Pb(II) ions with the interfering anion concentration is shown by Fig. 6B.

It was noticed that the presence of anions such as chloride and sulfate with in the concentration range 5-40 ppm had no significant effect on the removal of Pb(II) ions by magnetite (The removal percent is 99.4 and 99.0 % in case of chloride and sulfate, respectively). The percent removal decreased with increasing phosphate anions concentration (93.5% for 100 ppm phosphate solution). It was reported by Zhang et al. that high concentrations of phosphate in water decrease the sorption capacity of iron oxide [40].

Adsorption of heavy metals from real samples

Three real samples were collected from two different places, south Delta and central Delta of the Nile River. Sample (1) is simply tap water obtained from 6th October City (south Delta), sample (2) is a wastewater obtained from a nearby factory in 6th October City (south Delta) and sample (3) is a waste-water sample obtained from a given factory nearby Kafr El Zayat City (central Delta, 111 km north from Cairo). The Pb(II) ion was estimated in the three samples and it was found that samples (1) and (2) contained traces of Pb(II) ions (less than 1 ppb), while sample (3) had the relatively highest Pb(II) ions concentration (1.338ppm). Adsorption test for Pb(II) ions removal by magnetite was performed in all samples and the remaining Pb(II) ion concentration in each sample was estimated. It

was found that less than 1 ppb of Pb(II) ions can be detected after adsorption, suggesting the effective performance of magnetite as a sorbent for Pb(II) ions removal in the presence of the real sample matrix, especially for sample (3).

Moreover, sample (3) was spiked with different Pb(II) ion concentrations to investigate the adsorption isotherm and the magnetite capacity in the real sample, taking into consideration the matrix effect. The value of the magnetite adsorption capacity was found to be 526.32 mg/g, which is comparable with the value

calculated from Langmuir isotherm performed in deionized water (576.37 mg/g, see Table 1). It can be concluded that the performance ability of magnetite sorbent is not affected by the matrix effect of the wastewater sample. In other words, it will be effective to apply magnetite as a sorbent for field removal of the Pb(II) ions.

Simultaneous determination of a ternary mixtures of Pb(II), Cd(II) and Cr(III) ions-containing solution

The effect of competing cations was previously studied, however all investigated cations are naturally occurring alkali or alkaline earth metal ions such as Na(I), Mg(II) and Ca(II) ions. In this section, the effect of competing transition metal

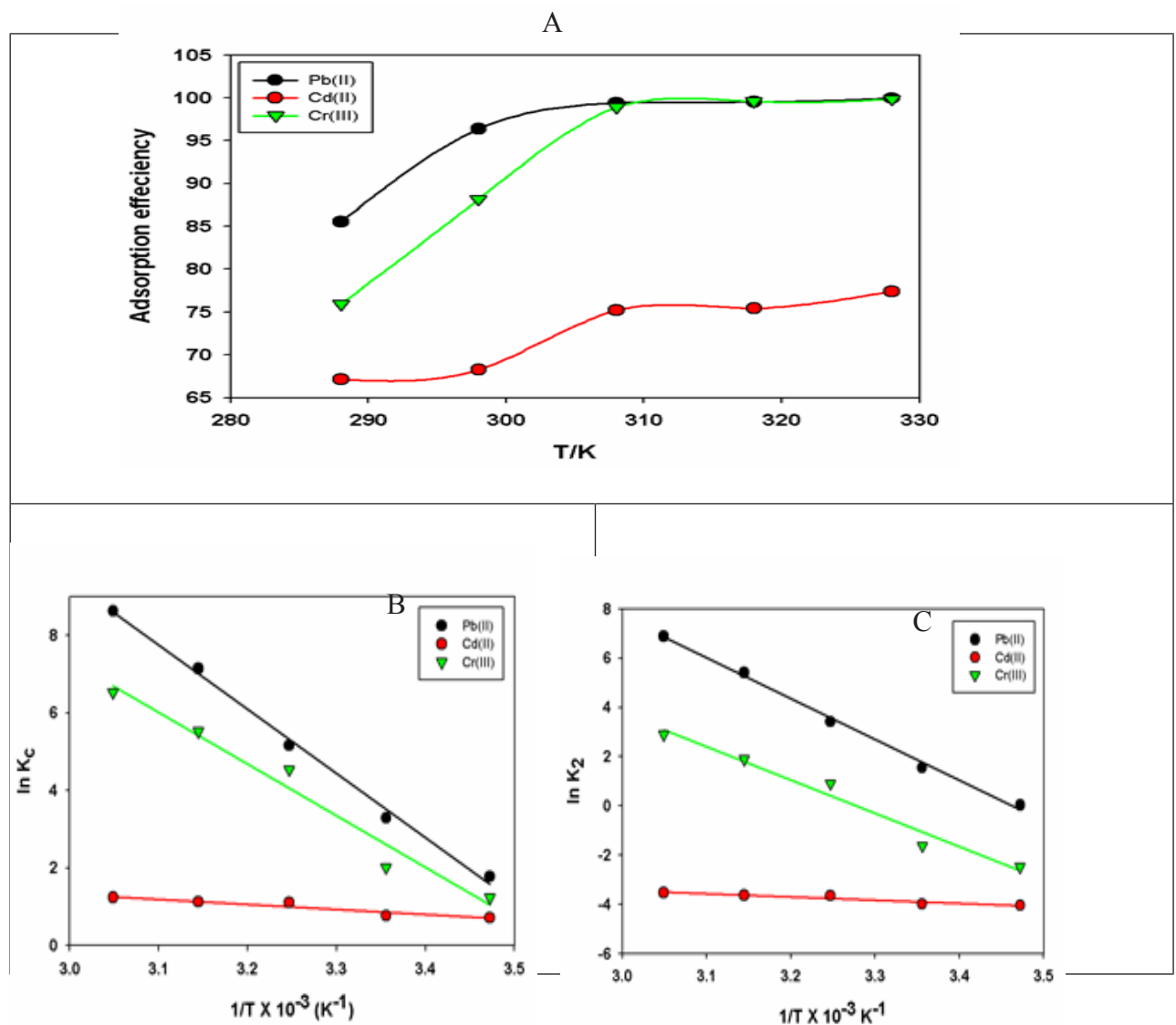


Fig. 5. (A) The temperature effect on the adsorption efficiency of magnetite toward different metal ions, (B) Transition-state and (C) Arrhenius plots.

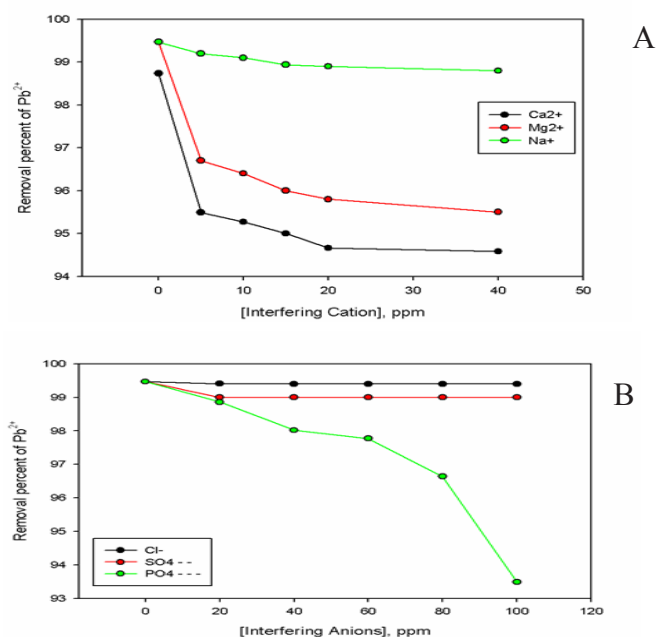


Fig. 6. Effect of (A) competing cations, (B) interfering anions on lead ion removal by magnetite.

ions such as Pb(II), Cd(II) and Cr(III) ions that may co-exist in wastewater on the adsorption ability of magnetite toward each metal ion will be focused. The adsorption test was carried out in a ternary Pb(II), Cd(II) and Cr(III) ions-containing solution where each metal ion has an initial concentration of 15 ppm. Table 4 shows a comparison between the removal percent of each of the three investigated metal ions by magnetite in individual and ternary solutions.

It can be noticed that the adsorption ability of the magnetite for each metal ion is almost unaffected.

Regeneration and reuse of magnetite

Desorption of metal ions can be achieved using mineral acids, salt solutions and bases. In this study the desorption of Cd(II) ions from magnetite surface was carried out by nitric acid solution. In the first adsorption test, a freshly prepared magnetite was used and the removal percent of Cd(II) ions was 77.3 %. The used magnetite was then filtrated, dried, added to 100ml of 1% HNO₃ to achieve the desorption test. The recovery percent of Cd(II) ions was 91.4% of the total adsorbed amount. This high value reflects the possibility to apply nitric acid successfully for the magnetite regeneration. A trace of Fe(III) ions was detected in the recovery solution (less than 1 % of the total iron used in

magnetite preparation), thus nitric acid can be used to regenerate magnetite without considerable loss of iron content.

The adsorption ability of the regenerated magnetite was also investigated by performing the second adsorption test and the removal percent of Cd(II) ions was 65.0 %. This resulted in a decrease in the sorption capacity during repetition of the adsorption test of about 6.18 %. The small decrease in the sorption capacity suggests the successful reuse of the regenerated magnetite.

TABLE 4. A comparison between the removal percent of magnetite toward studied metal ions, in individual and ternary solutions.

Metal ion	Removal % in individual solution	Removal % in ternary solution
Pb(II)	98.8	98.0
Cd(II)	89.4	88.8
Cr(III)	99.9	99.6

Conclusions

It was Nano-magnetite (Fe₃O₄) was successfully synthesized using eco-friendly method. Following a Langmuir model the sorption capacities for Pb(II), Cd(II) and Cr(III) ions from water and wastewater are 576.4, 144.3 and 301.0

TABLE 1. Calculated parameters from Freundlich and Langmuir models parameters for the adsorption of Pb(II), Cd(II) and Cr(III) on magnetite.

Metal ion	Freundlich			Langmuir		
	K (mg/g)	n (g/L)	R^2	K_L (mg/g)	b (L/mg)	R^2
Pb(II)	108.85	1.44	0.9158	576.37	0.37	0.9753
Cd(II)	33.78	2.11	0.9682	144.34	0.28	0.9970
Cr(III)	307.97	2.46	0.8322	301.02	12.72	0.9922

TABLE 2. Comparison between adsorption capacity values of magnetite and other sorbents.

Metal ion	Adsorbent	Adsorption capacity (mg/g)	Reference
Pb (II)	Activated carbon	43.8	[9]
	Natural clinoptilolite	166.0	[10]
	Activated Firmiana simplex leaf	379.3	[11]
	SiO ₂ /graphene	113.6	[12]
	Polyampholyte	202.0	[13]
	PS-EDTA resin	32.1	[14]
	K. birnessite	164.3	[15]
	Nano-Fe ₃ O ₄	576.4	This study
Cd (II)	12 M-HCl-treated palygorskite	12.9	[16]
	Nano-CuFe ₂ O ₄	17.5	[17]
	H ₂ SO ₄ -treated wheat bran	43.1	[18]
	MnO ₂ loaded D301 resin	77.8	[19]
	Chitin	14.0	[20]
	Hematite	4.9	[21]
	Bone char	64.1	[22]
	Orange waste	48.3	[23]
	Humic acid/sod. Alginate	148.9	[24]
	Polyampholyte	182.0	[13]
	Nano-Fe ₃ O ₄	144.3	This study
Cr (III)	Polyvinylalc/sod. alginate	59.9	[25]
	EDHPA onto Amberlite XAD7	3.0	[26]
	Hydrous TiO ₂	5.0	[27]
	Activated carbon	19.2	[28]
	Lignocellulosic waste	285.7	[29]
	Filtrisorb 400	30	[30]
	Nano-Fe ₃ O ₄	301.0	This study

TABLE 3. Calculated thermodynamics parameters for the adsorption of Pb(II), Cd(II) and Cr(III) on magnetite.

Metal ion	ΔH° (kJ/mol)	ΔS° (kJ/mol.K)	ΔG_0 (kJ/mol)				
			15°C	25°C	35°C	45°C	55°C
Pb(II)	124.41	0.4460	-4.25	-8.13	-13.19	-18.85	-23.49
Cd(II)	10.95	0.0438	-1.71	-1.89	-2.84	-2.96	-3.35
Cr(III)	110.84	0.3936	-2.94	-4.98	-11.60	-14.58	-17.77

mg/g, respectively. The activation energy values for Pb(II), Cd(II) and Cr(III) suggested chemical adsorption for the first and third cations, while the second followed a physical type adsorption. The presence of Ca(II) and Mg(II) cations and phosphate anions affect the adsorption process. Pb(II) removal (526.3 mg/g) from waste-water sample from the Nile River was successful. Regeneration of the used magnetite was possible

using 1% nitric acid with 91.4% recovery.

Acknowledgement

The authors would like to acknowledge the financial support from Cairo University through the Vice President Office for Research Funds.

References

- Wang, E., Guo, Y., Yang, L., Han, M., Zhao, J. and Cheng, X., Nanomaterials as sorbents to remove heavy metal ions in wastewater treatment. *J. Environ. Anal. Toxicol.* **2**, 2-7 (2010).
- Kumari, M., Pittman, Jr.C.U. and Mohan, D., Heavy metals [chromium (VI) and lead (II)] removal from water using mesoporous magnetite (Fe₃O₄) nanospheres. *J. Colloid Interface Sci.* **442**, 120-132 (2015).
- Chowdhury, S.R. and Yanful, E.K., Kinetics of cadmium (II) uptake by mixed maghemite-magnetite nanoparticles. *J. Environ. Manage.* **129**, 642-651 (2013).
- Chowdhury, S.R. and Yanful, E.K. Arsenic and chromium removal by mixed magnetite-maghemite nanoparticles and the effect of phosphate on removal. *J. Environ. Manage.* **91**, 2238-2247 (2010).
- Ahmed, M.A., Ali, S.M., El-Deka, S.I. and Galal, A., Magnetite-hematite nanoparticles prepared by green methods for heavy metal ions removal from water. *Mater. Sci. Eng.* **B178**, 744-751 (2013).
- Cullity, B.D., *Elements Of X-Rays Diffraction*. Wiley, USA (1978).
- Boparai, H.K., Joseph, M. and O'Carroll, D. M., Kinetics and thermodynamics of cadmium ion removal by adsorption onto nanozerovalent iron particles. *J. Hazard. Mater.* **186**, 458-465 (2011).
- Yang, C.H., Statistical mechanical study on the Freundlich isotherm equation. *J. Colloid Interface Sci.* **208**, 379-387 (1998).
- Acharyaa, J., Sahub, J.N., Mohantyc, C.R. and Meikapb, B.C., Removal of lead (II) from wastewater by activated carbon developed from Tamarind wood by zinc chloride activation. *Chem. Eng. J.* **149**, 249-262 (2009).
- Bekta, N. and Kara, S. Removal of lead from aqueous solutions by natural clinoptilolite: equilibrium and kinetic studies. *Sep. Purif. Technol.* **39**, 189-200 (2004).
- Li, Z., Tang, X., Chen, Y., Wei, L. and Wang, Y. Activation of Firmiana Simplex leaf and the enhanced Pb(II) adsorption performance: Equilibrium and kinetic studies. *J. Hazard. Mater.* **169**, 386-394 (2009).
- Hao, L., Song, H., Zhang, L., Wan, X., Tang, Y., and Lv, Y., SiO₂/ graphene composite for highly selective adsorption of Pb(II) ion. *J. Colloid Interface Sci.* **369**, 381-387 (2012).
- Copello, G.J., Dioz, L.E. and Dall'Orto, V.C. Adsorption of Cd(II) and Pb(II) onto a one step-synthesized polyampholyte: Kinetics and equilibrium studies. *J. Hazard. Mater.* **217-218**, 374-381 (2012).
- Wang, L., Yang, L., Li, Y., Zhang, Y., Ma, X. and Ye, Z., Study on adsorption mechanism of Pb(II) and Cu(II) in aqueous solution using PS-EDTA resin. *Chem. Eng. J.* **163**, 364-372 (2010).
- Eren, E., Gumus, H. and Sarihan, A., Synthesis, structural characterization and Pb(II) adsorption behavior of K- and H-birnessite samples. *Desalination*, **279**, 75-85 (2011).
- Wang, W., Chen, H. and Wang, A., Adsorption characteristics of Cd(II) from aqueous solution onto activated palygorskite. *Sep. Purif. Technol.* **55**, 157-164 (2007).
- Tu, Y., You, C. and Chang, C., Kinetics and thermodynamics of adsorption for Cd on green manufactured nano-particles. *J. Hazard. Mater.* **235-236**, 116-122 (2012).
- Ozer, A. and Pirincci, H.B., The adsorption of Cd(II) ions on sulphuric acid-treated wheat bran. *J. Hazard. Mater.* **137**, 849-855 (2006).
- Zhiliang, Z., Hongmei, M.A., Ronghua, Z., Yuanxin, G.E. and Jianfu, Z., Removal of cadmium using MnO₂ loaded D301 resin. *J. Environ. Sci.* **19**, 652-656 (2007).
- Benguella, B. and Benaissa, H., Cadmium removal from aqueous solutions by chitin: kinetic and equilibrium studies. *Water Res.* **36**, 2463-2474 (2002).
- Singh, D.B., Rupainwar, D.C., Prasad, G. and Jayaprakas, K.C., Studies on the Cd(II) removal from water by adsorption. *J. Hazard. Mater.* **60**, 29-40 (1998).

22. Cheung, C.W., Porter, J.F. and McKay, G., Sorption kinetic analysis for the removal of cadmium ions from effluents using bone char. *Water Res.* **35**, 605-612 (2001).
23. Perez-Marin, A.B., Zapata, V.M., Ortuno, J.F., Aguilar, M., Saez, J. and Llorens, M., Removal of cadmium from aqueous solutions by adsorption onto orange waste. *J. Hazard. Mater.* **139**, 122-131 (2007).
24. Chen, J.H., Ni, J.C., Liu, Q.L. and Li, S.X., Adsorption behavior of Cd(II) ions on humic acid-immobilized sodium alginate and hydroxyl ethyl cellulose blending porous composite membrane adsorbent. *Desalination*, **285**, 54-61 (2012).
25. Chen, J.H., Li, G.P., Liu, Q.L., Ni, J.C., Wu, W.B. and Lin, J.M., Cr(III) ionic imprinted polyvinyl alcohol/sodium alginate (PVA/SA) porous composite membranes for selective adsorption of Cr(III) ions. *Chem. Eng. J.* **165**, 465-473 (2010).
26. Ciopec, M., Davidescu, C.M., Negrea, A., Grozav, I., Lupa, L. and Negrea, P., Adsorption studies of Cr(III) ions from aqueous solutions by DEHPA impregnated onto Amberlite XAD7 – Factorial design analysis. *Chem. Eng. Res. Des.* **90**, 1660-1670 (2012).
27. Tel, H., Altas, Y. and Taner, M.S., Adsorption characteristics and separation of Cr(III) and Cr(VI) on hydrous titanium(IV) oxide. *J. Hazard. Mater.* **112**, 225-231 (2014).
28. Rivera-Utrilla, J. and Sanchez-Polo, M., Adsorption of Cr(III) on ozonised activated carbon. Importance of π -cation interactions. *Water Res.* **37**, 3335-3340 (2013).
29. Singh, K.K., Rastogi, R. and Hasan, S.H., Removal of Cr(VI) from wastewater using rice bran. *J. Colloid Interface Sci.* **290**, 61-68 (2005).
30. Park, J.S. and Jung, W.Y., Removal of chromium by activated carbon fibers plated with copper metal. *Carbon Sci.* **2**, 15-21 (2001).
31. Zhang, H., Tang, Y., Cai, D., Liu, X., Wang, X., Huang, Q. et al., Hexavalent chromium removal from aqueous solution by algal bloom residue derived activated carbon: Equilibrium and kinetic studies. *J. Hazard. Mater.* **181**, 801-808, (2010).
32. Wang, X.S., Chen, L.F., Li, F.Y., Chen, K.L., Wan, W.Y. and Tang, Y.J., Removal of Cr(VI) with wheat-residue derived black carbon: reaction mechanism and adsorption performance. *J. Hazard. Mater.* **175**, 816-822 (2010).
33. Mohanty, K., Jha, M., Meikap, B.C. and Biswas, M.N., Removal of chromium (VI) from dilute aqueous solutions by activated carbon developed from Terminalia arjuna nuts activated with zinc chloride. *Chem. Eng. Sci.* **60**, 3049-3059 (2005).
34. Acharyaa, J., Sahub, J.N., Sahoob, B.K., Mohantyc, C.R. and Meikap, B.C., Removal of chromium(VI) from wastewater by activated carbon developed from Tamarind wood activated with zinc chloride. *Chem. Eng. J.* **150**, 25-39 (2009).
35. Celik, M.S. and Yoon, R.H., Adsorption of Poly(oxyethylene)-nonylphenol homologues on a low-ash coal. *Langmuir.* **7**: 1770-1774 (1991).
36. Mouflih, M., Aklil, A., Jahroud, N., Gourai, M. and Sebti, S., Removal of lead from aqueous solutions by natural phosphate. *Hydrometallurgy.* **81**, 219-225 (2006).
37. Unuabonah, E.I., Adebowale, K.O. and Olu-Owolabi, B.I., Kinetic and thermodynamic studies of the adsorption of lead (II) ions onto phosphate-modified kaolinite clay. *J. Hazard. Mater.* **144**, 386-395 (2007).
38. Ozcan, A., Ozcan, A.S. and Gok, O., Adsorption kinetics and isotherms of anionic dye of reactive blue 19 from aqueous solutions onto DTMA-sepiolite, in: A.A. Lewinsky (Ed.), *Hazardous Materials and Wastewater—Treatment, Removal and Analysis*, Nova Science Publisher, New York (2007).
39. Marcus, Y., Thermodynamics of solvation of ions: part 5-Gibbs free energy of hydration at 298.15 K. *J. Chem. Soc. Faraday Trans.* **87**, 2995-2999 (1991).
40. Zhang, W., Singh, P., Paling, E. and Delides, S., Arsenic removal from contaminated water by natural iron ores. *Minerals Eng.* **17**, 517-524 (2004).

(Received : 2 / 11 / 2016
Accepted : 23 / 4 / 2017)

ازالة ايونات المعادن الثقيلة الضارة من مياه الصرف الصحي بواسطة النانو ماجنتيت : دراسة حالة بمياه نهر النيل

شيماء علي، أحمد جلال، ندا عطا و ياسمين شماخ
قسم الكيمياء- كلية العلوم- جامعة القاهرة- الجيزة -12613 مصر

تم استخدام النانو ماجنتيت كمادة ادمصاص صديقة للبيئة (بدون استخدام الرغويات) لازالة ايونات الرصاص، الكاديوم والكروم من مياه الصرف. تم استخدام الاشعة السينية الحبيدية و المجهر الالكتروني النافذ عالي الدقة لتأكيد تكون بنية تكعيبية احادية المرحلة، و اظهرت صور المجهر الالكتروني الماسح تجمع من جسيمات الماجنتيت بعد الادمصاص. و قد اظهر متعادل لانجيمير الحراري قدرات ادمصاص قصوى تصل الى 576.4، 144.3 و 301.0 ملجم/جم لايونات الرصاص، الكاديوم والكروم على التوالي. ووجد ان الية الادمصاص تتبع التفاعلات الحركية الشبه ثنائيةالدرجة . اظهرت دراساتاثير الكاتيونات و الانيونات المناقسة اثار طفيفة على معدل الادمصاص. اظهر الماجنتيت ذو قدرة الادمصاص العالية القدرة على ادمصاص ايونات الرصاص، الكاديوم والكروم من خليط ثلاثي بنفس الكفاءة كما هو الحال في الادمصاص من المحاليل احادية الايونات. يمكن اعادة تدوير الماجنتيت باستخدام حمض النيتريك (1%) بدرجة من الكفاءة 91.4% و استخدامه مرة اخرى بنسبة كفاءة اداء 84.1% مقارنة بالماجنيتيت المحضر حديثا. كمثل على التطبيق، تم استخدام النانو ماجنتيت لتطهير عينات مياه من النهر تحتوي على ايونات الرصاص.